P-124: Study of Stacked Alignment Layers on a Single Substrate with Spatial Liquid Crystal Pretilt Angles and its Applications

Man-Chun Tseng, Chung-Yung Lee, Yuet-Wing Li, and Hoi-Sing Kwok

Center for Display Research, Department of Electrical and Electronic Engineering
Hong Kong University of Science and Technology
Clear Water Bay, Kowloon, Hong Kong

Abstract

In this paper, we report recent developments in stacked alignment to generate spatially varying liquid crystal pretilt angles. This is a nanostructure alignment surface that can be produces any pretilt angle on a single substrate. The pretilt angle's profile can be controlled. An electrically tunable liquid crystal lens using such nanostructure alignment surface is demonstrated

1. Introduction

Pretilt angle generation and liquid crystal alignment is a major factor in improving characteristics of LCD. New nanostructured alignment surfaces have attracted some attention in recent years [1-3]. Many LCDs are based on either planar alignment or vertical alignment. It is difficult to obtain pretilt angles in range of 20º-70º. Various applications are possible if such intermediate pretilt angle region can be easily obtained. For instance, such high pretilt angle can be applied to bistable display devices [4] and no-bias-bend fast switching display devices [5].

Study of heterogeneous surface for liquid crystal alignment has witnessed a rapid growth in recent years. [6-8] We recently demonstrated a stack alignment surface that is capable of generating arbitrary pretilt angles and azimuth angles for liquid crystal by controlling the domain ratio of the upper photo alignment layer using dewetting [9]. In this paper, we demonstrate that based on the self-organized dewetting technique, further control of the domain ratio is possible by varying the UV dosage of the photo alignment layer. The alignments produced are robust since various pretilt angles can be generated on the same substrate by designing the UV light beam spatial profile.

2. Methodology

The structure of the proposed spatially stacked alignment layers (SSAL) is shown in Figure 1. SSAL consists of two domains. One is a single continuous alignment layer and the other one is a top alignment layer which can be either continuous or discontinuous as controlled by dewetting. This type of alignment surfaces generally comprises two kinds of domains favoring different liquid crystal orientations.

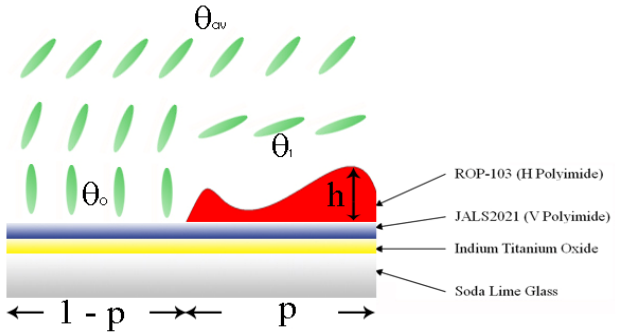

Figure 1. An overview of the proposed stacked alignment structure

If each type of domain has surface energy $W_i(\theta,\phi)$, where $i=1,2$, the unit-area surface energy F_s can be written as [10]

$$F_{s(av)}\left(\theta_{av}(r),\phi_{av}(r)\right)=\delta(z)\sum_{i=1}^{2}a_i(x,y)F_i\left(\theta_i(r),\phi_i(r)\right)$$

where $r=(x,y,z)$ is a position vector in the simulation cell and the liquid crystal director field is denoted by $n(r)\equiv(\cos\theta\cos\phi,\cos\theta\sin\phi,\sin\theta)$. $\theta_i(r)$ and $\phi_i(r)$ are the pretilt angles and azimuth angles of the liquid crystal director respectively. $a_i(x,y)$ equals to one if (x,y) belongs to domain i and zero otherwise so that the area fraction of domain i is obtainable by integrating $a_i(x,y)$ over the $z=0$ unit surface.

Suppose the area fraction of the top discontinuous layer is p. The bottom single continuous alignment section surface energy can be represent by Rapini-Papoular form

$$F_0(\theta_0)=\frac{1}{2}W_0\sin^2(\theta_{av}-\theta_0)$$

The surface energy of the top stacked alignment section is

$$F_1(\theta_1)=W_t\sin^2(\theta_1-\theta_t)+D^{-\eta}[W_b\sin^2(\theta_1-\theta_b)]$$

Where θ_0 is the single continuous alignment layer pretilt angle which is equal to bottom alignment layer pretilt angle θ_b, θ_1 is the stacked alignment pretilt angle, θ_{av} is the resultant average pretilt angle and the θ_t is the top alignment layer pretilt angle. The screening effect can be approximated by the anisotropic "van der

Waals-like interaction" form: $D^{-\eta} = h^{-3}$, where h is the thickness of the stacked alignment layer.

We let both W_t and W_b to be $1x10^{-3}$ Jm^{-2}, $\theta_t = 2^0$ and $\theta_b = 85^0$ respectively. The Frank elastic constants are k_{11} = 14pN, k_{22} = 7pN, k_{33} = 19pN. The simulation result is shown in Figure 2.

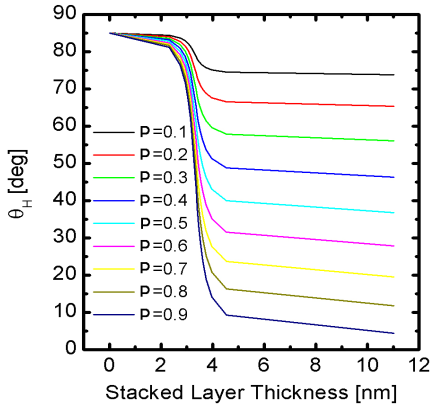

Figure 2. The effect of Stacked layer Thickness on the homogenized pretilt angles

The surface energy F_1 dominates when p is close to 1, so that the pretilt angle decreases when the stacked layer thickness increase. The abrupt change of the pretilt angles is due to the third order screening effect.

3. Experiment and Results

The following describes the details of the experiment procedure. Firstly, a vertical alignment polyimide JALS2021 from JSR Corporation was spin coated on an ITO glass substrate. Figure 3 shows the AFM picture of the vertical alignment polyimide after the baking.

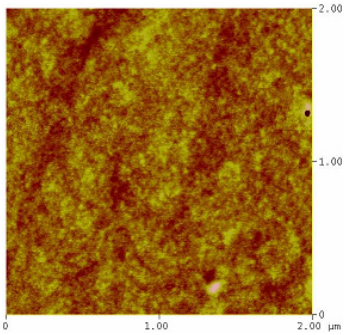

Figure 3. AFM picture of the continuous vertical alignment layer

The vertical alignment polyimide was a continuous layer since it completely covered the ITO crystalline pattern. The vertical alignment polyimide was then rubbed to obtain the first principle pretilt angle θ_0 (θ_0=85°). Then, a photo alignment material: ROP-103 from Rolic Ltd was spin coated on top of the polyimide. The photoalignment layer was exposed with different duration by a linearly polarized light with a wavelength of 340nm.

Since some of the ROP-103 was not fully polymerized due to the short UV exposure time, the un-polymerized photo alignment material was rinsed away by the solvent. Figure 4 shows the AFM picture of ROP-103 photo alignment polyimide under different exposed time.

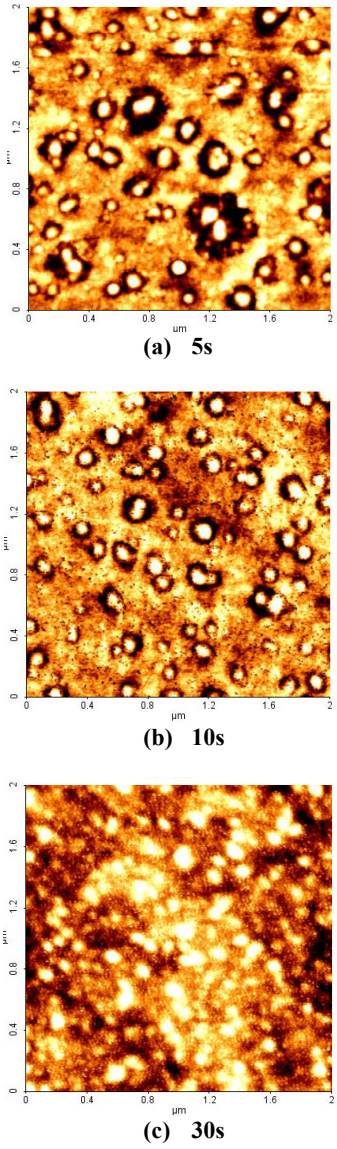

(a) 5s

(b) 10s

(c) 30s

Figure 4. AFM picture of ROP-103 photo alignment polyimide with a 0.125% by under different exposed time

The longer the exposed time, the more photo alignment materials were polymerized and remained so that a thicker photo alignment was obtained. In addition, the sizes of domain which were formed by dewetting also varied accordingly with UV dosage. It is because the slope of the domain edge is not a delta function but possesses a curvature. The variation of domain sizes also can be proved by the roughness of the SSAL surface which is shown in Figure 5(a). It can be seen that the roughness drop as the exposure energy increases. A coarse surface implies to a large domain surface.

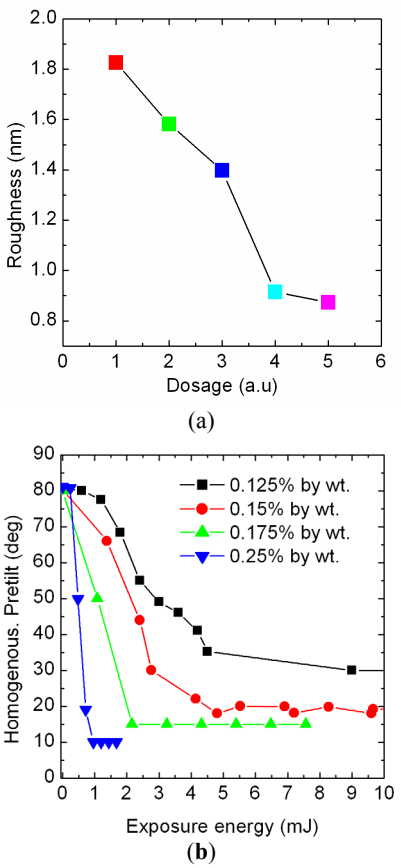

Figure 5. (a)Surface Roughness of SSAL versus UV dosage (b)Homogenized pretilt angle versus exposure energy

The resultant pretilt angles versus different exposure energies are shown in Figure 5(b). The pretilt angles were measured by the crystal rotation method [11]. It can be seen that the resultant pretilt angles drop as the exposure energy increases. When there is no dewetting likes the highest concentration upper alignment layer curve (0.25% by wt), it behaves like a continuous layer. The rapid drop of pretilt angles is only due to the third order screening effect which matches the simulation. When the dewetting occur, domain sizes are formed and controlled by the UV dosage. The third order screening effect is weaken by domains occur so that the pretilt angles drop more tardily. This is encouraging since the pretilt angles can be more precise controlled spatially by controlling the exposure UV profile. Some test cells with different pretilt angles are fabricated which are shown in Figure 6.

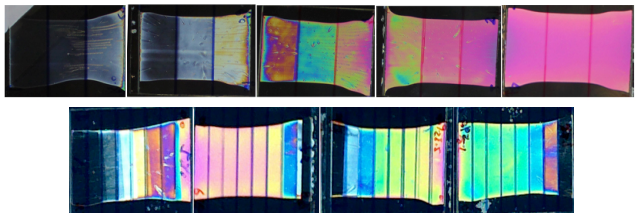

Figure 6. Test cells for homogenized pretilt angle under different UV exposure energy

4. Applications

Obviously, many high pretilt display devices such as bistable display devices, no-bias-bend fast switching display devices can be fabricated. In here, we show results for a tunable focal length lens. The proposed structure is shown in Figure 7. The upper cell alignment layer was a single vertical alignment layer which gave high pretilt angles. The bottom cell alignment layer was a SSAL. This result in a HAN cell structure since the retardation is quite linear to the pretilt angle in HAN cell structure.

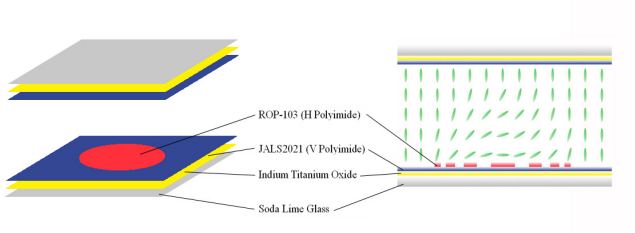

Figure 7. An overview of the proposed LC variable-focus lens

The fabrication processes which are shown in Figure 8 are almost the same to the above discussion of the SSAL in section 3.

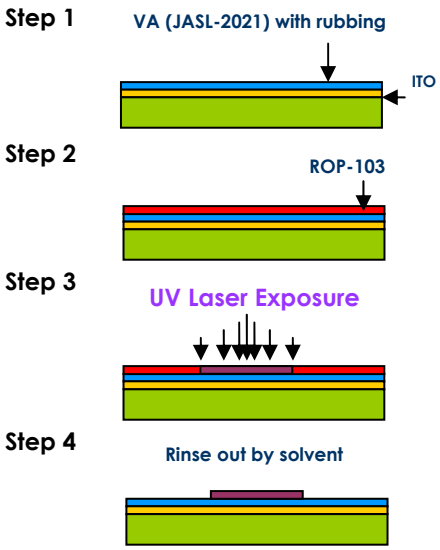

Figure 8. Process flow of the bottom cell fabrication

In step 3, instead of controlling the UV dosage by exposure time, a 325nm wavelength UV laser with a disc shape Gaussian intensity profile was adopted to pattern the lens profile. The closer to the centre of the laser spot, the more photo alignment material would be polymerized within a fixed duration. The denser the polymerized photo alignment surface, the lower pretilt angle was obtained. The un-polymerized photo alignment material including the one outside the laser spot will be rinse away. A disc-shape spatially distributed pretilt angle could be formed. This LC lens exhibited a focusing function without a voltage application and its focal length was electrically controllable. Both top and bottom substrates were placed in an anti-parallel rubbing direction of the vertical alignment layer and

were sandwiched by a pair of parallel polarizers which are parallel to the rubbing direction. The cell gap was 16μm and the liquid crystal E7 from Merck was used to fill into the cell because of its high Δn (~0.27).

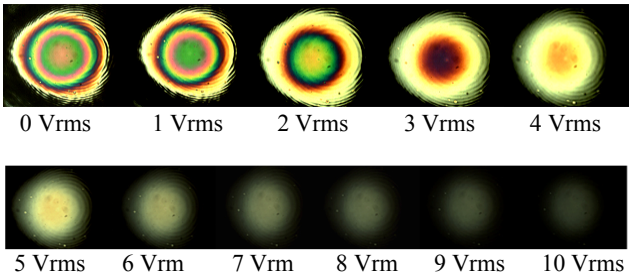

Figure 9. Interference fringes change at 0 - 10 Vrms with a 1 kHz frequency

The lens properties were observed by an interference method. An AC voltage with 1 kHz frequency was applied across the ITO electrodes. Figure 9 shows the observed fringe patterns under different voltages. The interference fringe number was the highest without voltage application and it was decreased with voltage. A nearly plane wave was observed when 3Vrms was applied.

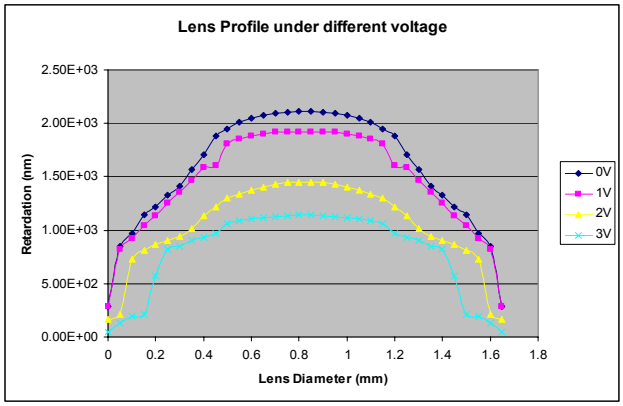

Figure 10. Phase retardation profile at various values of applied voltage

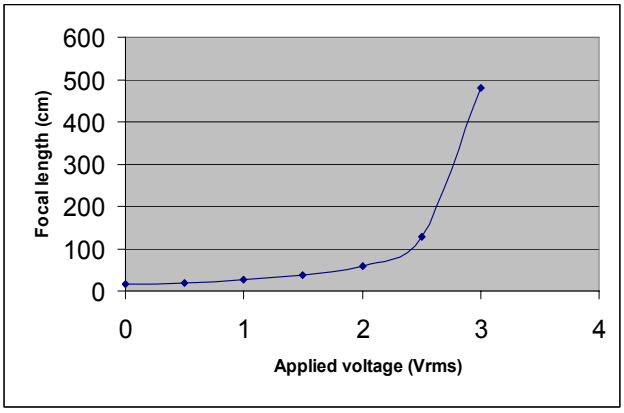

Figure 11. Focal lengths at various values of applied voltage

Figure 10 shows the phase retardation at 0-3 Vrms which was measured by the interference method. The gradient of phase retardation became smaller when the voltage increased. The focal length became smaller when the applied voltage increased as shown in Figure 11. The shortest focal length is about 15cm when no voltage is applied.

5. Conclusion

We have demonstrated an alignment surface (SSAL) that is capable of patterning arbitrary pretilt angles spatially for a liquid crystal layer. It is achieved by stacking two alignment materials where the top layer is a photoalignment material. Thus the spatial profile of the pretilt angle can be controlled by the spatial profile of the UV source. A variable-focus liquid crystal lens was achieved by SSAL. SSAL can be applied to many new optical applications such tunable optical elements and 3D displays. Such alignment layer is particularly useful for high pretilt angles or multi-domain applications, bistable displays, fast switching displays, optical or waveguide devices.

6. Acknowledgement

The research was support by the Hong Kong Government Research Grants Council Grant Number 614807.

7. References

[1] Xuemin Lu, Fuk Kay Lee, Ping Sheng, H. S. Kwok, V. Chigrinov and Ophelia K. C. Tsui, Appl. Phys. Lett., **88**, 243508, 2006

[2] Fion S. Y. Yeung, F. C. Xie, Jones T. K. Wan, F. K. Lee, Ophelia K. C. Tsui, P. Sheng and H. S. Kwok, J. Appl. Phys., **99**, 124506, 2006

[3] You-Jin Lee, Jin Seog Gwag, Young-Ki Kim, and Jae-Hoon Kim, IDRC, 08 ,173-176, 2008

[4] X. J. Yu and H. S. Kwok, SID04 Digest, Vol. XXXV, 875-877, 2004

[5] Fion S. Y. Yeung and H. S. Kwok, Appl. Phys. Lett., **88**, 063505, 2006

[6] Ke Zhang, Na Liu, Robert J. Twieg, Brian C. Auman, Philip J. Bos, Liq. Cryst. **27**, pp. 1191-1197, 2008

[7] J.Kim, M. Yoneya, and H. Yokoyama, Nature(London) 420,159, 2002

[8] O.K.C. Tsui, F.K.Lee, B.Zhang, and P.Sheng, Phys. Rev. Lett. 91, 215501, 2003

[9] Hoi-Sing kwok and Yuet-Wing Li, IDRC, P133, 2009

[10] J. T. K. Wan, O. K. C. Tsui, H. S. Kwok, P. Sheng, Phys. Rev. E, 72, 021711, 2005

[11] Shirota, Koichiro; Yaginuma, Michio; Ishikawa, Ken; Takezoe, Hideo; Fukuda, Atsuo; Jap. J. Appl. Phys., **34**, 9A, 4905-4908, 1995